ACS Macro Letters

pubs.acs.org/macroletters Letter

Targeted Microfluidic Manufacturing to Mimic Biological Microenvironments: Cell-Encapsulated Hollow Fibers

Marilyn C. McNamara, Saurabh S. Aykar, Reza Montazami, and Nicole N. Hashemi*

Cite This: *ACS Macro Lett.* 2021, 10, 732–736 Read Online

ACCESS | Metrics & More | Article Recommendations | Supporting Information

ABSTRACT: At present, the blood–brain barrier (BBB) poses a challenge for treating a wide range of central nervous system disorders; reliable BBB models are still needed to understand and manipulate the transfer of molecules into the brain, thereby improving the efficiency of treatments. In this study, hollow, cell-laden microfibers are fabricated and investigated as a starting point for generating BBB models. The genetic effects of the manufacturing process are analyzed to understand the implications of encapsulating cells in this manner. These fibers are created using different manufacturing parameters to understand the effects on wall thickness and overall diameter. Then, dopaminergic rat cells are encapsulated into hollow fibers, which maintained at least 60% live cells throughout the three-day observation period. Lastly, genetic changes tyrosine hydroxylase (TH) and tubulin beta 3 class III (TUBB-3) are investigated to elucidate the effects on cell health and behavior; while the TH levels in encapsulated cells were similar to control cells, showing similar levels of TH synthesis, TUBB-3 was downregulated, indicating lower amounts of cellular neurogenesis.

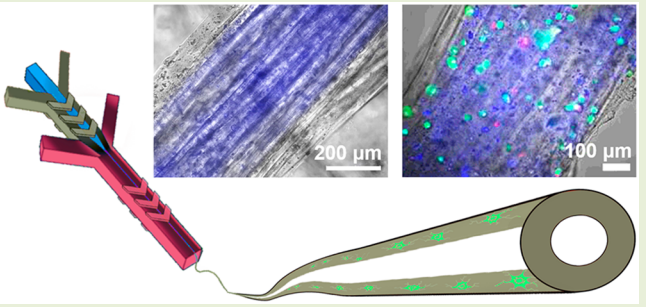

As the national and international population continues to grow older, age-related neuropathologies continue to be a tragic and expensive bane of modern times, with Alzheimer's alone projected to cost 1.1 trillion dollars per year by 2050,[1] while general neurological disorders account for 12% of the total global deaths.[2] Similarly, there is a dire need to treat other neurological disorders, such as mental illnesses, cancers, or traumatic brain injuries (TBIs), which are widespread and are detrimental to a wide age range.[3,4] In spite of this urgency, a currently insurmountable challenge has blocked efforts thus far; while it is crucial to protect the integrity of the central nervous system (CNS), the blood–brain barrier (BBB) blocks more than 98% of small molecules and all large molecules, thwarting almost all efforts to provide therapeutics to the brain.[5] Creating physiologically relevant BBB models is a crucial step to providing care for millions of patients across the globe, as it will allow for the rapid and reliable creation of effective neuropharmacological molecules.

The creation of a BBB model is a complicated undertaking. A physiologically relevant model must recreate the curvature found in the tubular BBB, while still allowing for the correct level of interstitial flow, as these factors affect the health and behavior of the endothelial cells that will be seeded onto the inside of the walls.[6] For instance, interstitial flow effects the proliferation rate, genetic expression, and orientation of the cells, and induces them to create tight gaps junctions that regulate active transport across the BBB.[7] Likewise, the diameter of the tube should be similar to those found in the human CNS, and should contain cell types that are relevant to the target tissues, like astrocytes, pericytes, and endothelial cells.

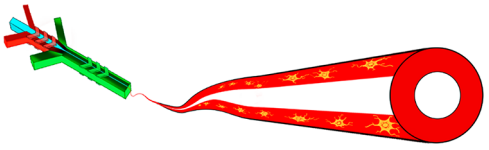

Figure 1. Schematic of hollow microfluidic microfiber manufacturing. A core fluid (blue) maintains an empty central channel throughout the microfluidic device. The alginate prepolymer (red) is mixed with N27 cells before manufacturing and is polymerized by ionic cross-linking through contact with $CaCl_2 \cdot 2H_2O$ in the sheath solution (green).

Hollow hydrogel fibers are prime candidates for creating cell-laden microfluidic structures that will mimic the micro-environment of the BBB. However, current work in creating cell-laden structures tends to underappreciate how the manufacturing process affects cells, which is a crucial factor

Received: March 9, 2021
Accepted: May 25, 2021
Published: May 28, 2021

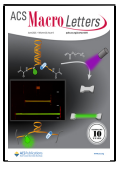

https://doi.org/10.1021/acsmacrolett.1c00159
ACS Macro Lett. 2021, 10, 732–736

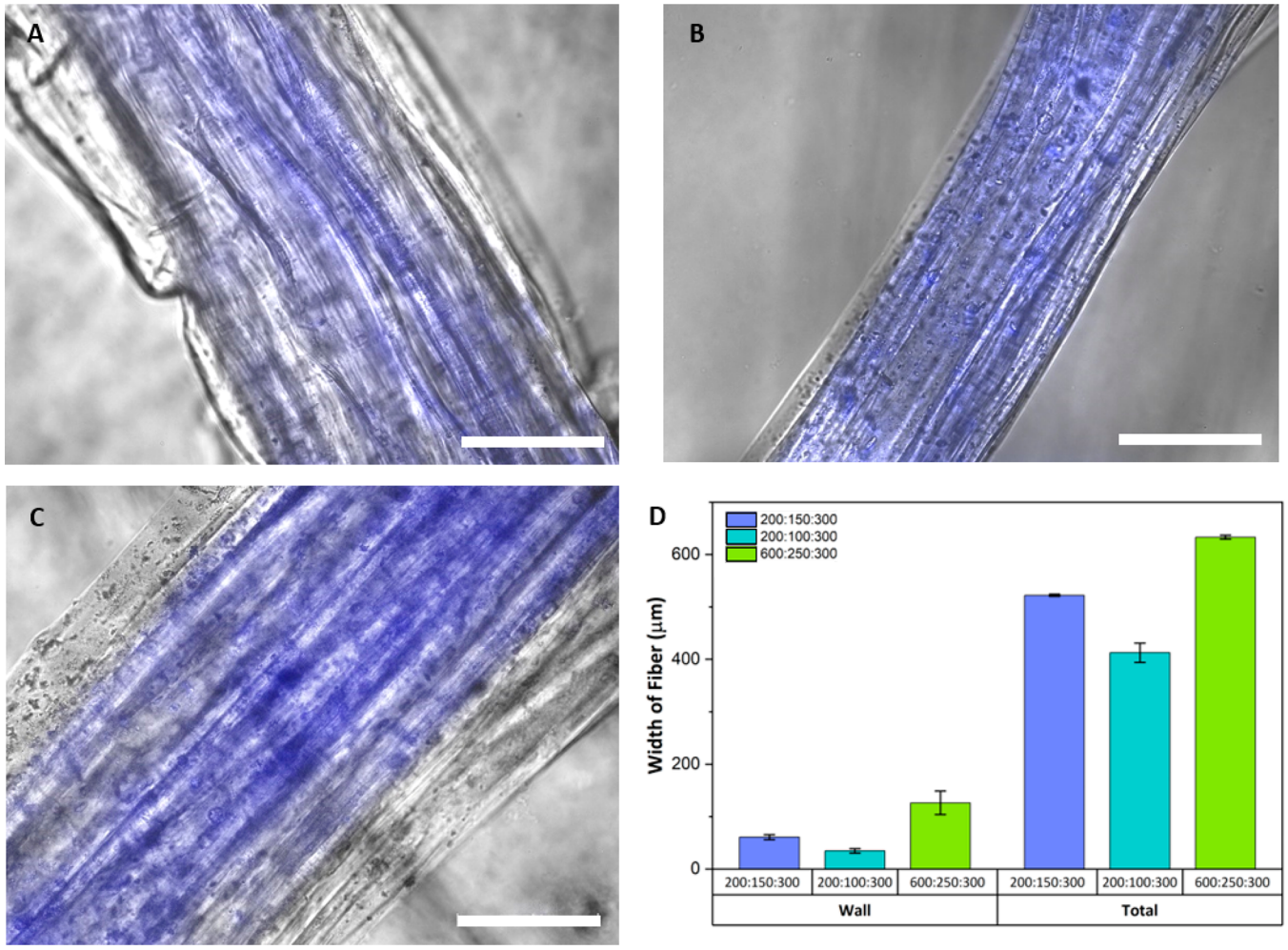

Figure 2. Sizes and topographies of hollow microfibers fabricated with different flow rate ratios. (A−C) Fluorescent imaging of hollow microfibers with CellTrackerCMTMR (orange, visualized here as blue) incorporated into the core fluid at manufacturing. Scale bars indicate 200 μm. (D) Wall and overall thickness of fibers made with different FRRs: (A) 200:150:300 μL/min; (B) 200:100:300 μL/min; (C) 600:250:300 μL/min ($n \geq 3$). Error bars represent ±1 standard deviation.

to consider when creating 3D cellular structures with high degrees of physiological relevancy. In this work, hollow microfibers were created using a five-inlet microfluidic device, which utilized chevrons in two locations to hydrodynamically shape the prepolymer fluid into a hollow microvessel.[8] Dopaminergic neural rat cells (N27s) were introduced into the prepolymer solution before gelation to understand the feasibility of the proposed manufacturing process and encapsulating cells into the walls of hollow fibers before further work, including endothelial cells. Their viability and initial genetic changes were analyzed shortly after encapsulation to understand the impact of the manufacturing process on cellular behavior.

Microfluidic devices are powerful tools for a variety of biomedical engineering applications, and they are unmatched for creating continuous, biocompatible hydrogel microfibers with highly controlled sizes and cross-sectional shapes.[9−15] Microfluidic fiber fabrication utilizes cell-safe gelation conditions, thereby enabling cell encapsulation, in direct contradiction to electrospinning.[16] Wetspinning, or extrusion, uses the same cell-safe gelation processes as microfluidics, but this system lacks the innovative internal geometries and hydrodynamic focusing that allow for the creation of fibers with a wide degree of sizes and cross-sectional shapes.[16] Additionally, the interaction of the solutions at the fluid−fluid boundary provides additional control over microstructures on the surface topography of the fibers.[17] The strength of this method enables the creation of bioinspired hydrogel microfibers for a variety of tissue targets, but the immediate cellular and genetic implications of microfluidic microfiber manufacturing remains understudied.

This method used a viscous core fluid, made of poly(ethylene glycol) (PEG) and gelatin, to create the hollow of the fiber (Figure 1). A prepolymer solution of alginate was introduced on either side, and upon entering the chevrons, the core fluid was hydrodynamically centered in the channel. Similarly, a sheath fluid containing PEG and calcium chloride dihydrate ($CaCl_2 \cdot 2H_2O$) was injected into the final set of inputs, further shaping the alginate microfiber while beginning the gelling process through ionic cross-linking.[16−19] The shape and size of the microfibers can be adjusted by changing the flow rates of the solutions or by using a microfluidic chip with different dimensions.[18,20−24] To ensure further solidification, the fibers were ejected into a $CaCl_2 \cdot 2H_2O$ collection bath before gathering and storing within maintenance media to ensure cell survival.[16,18,19] Degree of ionic cross-linking and the identity of the cross-linker can help modify the properties of the polymer, allowing for a high degree of control over the

https://doi.org/10.1021/acsmacrolett.1c00159
ACS Macro Lett. 2021, 10, 732−736

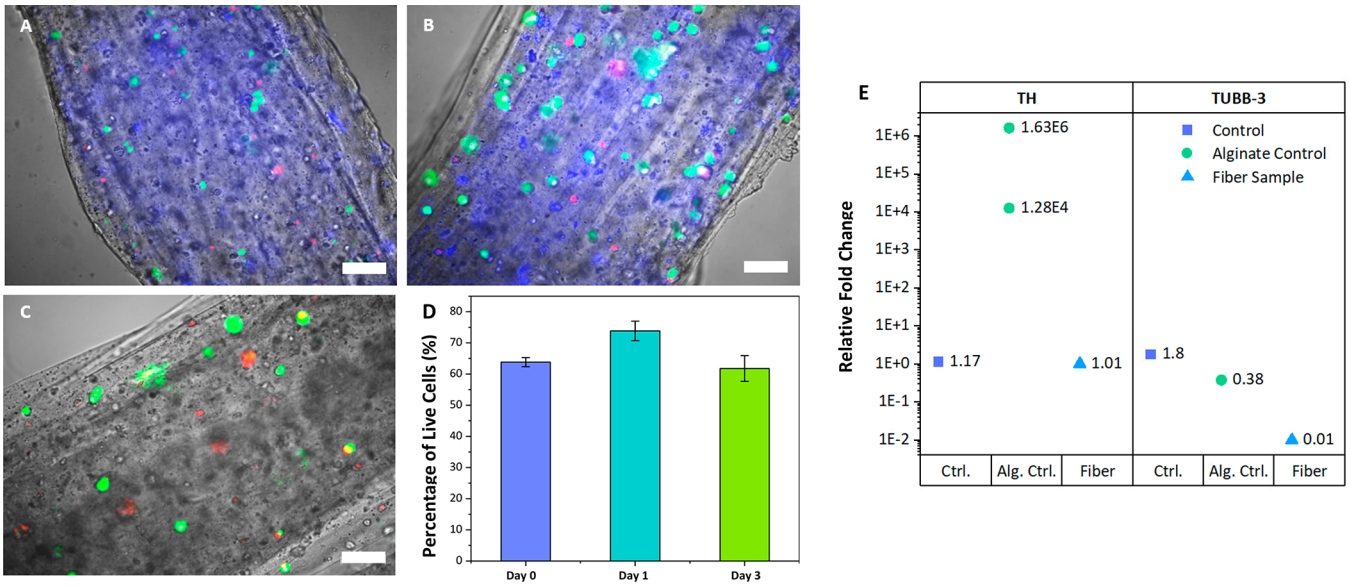

Figure 3. Viability and genetic responses of cells encapsulated into hollow alginate microfibers using a microfluidic manufacturing technique. (A–C) Fluorescent imaging of cell-laden hollow fibers made with a FRR of 600:250:300 μL/min immediately after fabrication (A), 1 day after fabrication (B), and 3 days after fabrication (C). Cells were stained immediately before imaging using CellTracker CMFDA (green) for live cells and propidium iodide (red) for dead cells. The hollow was stained at manufacturing using CellTracker CMTMR (orange), which is visualized as blue to easily distinguish the cells, and which lost fluorescence before day three. Scale bars indicate 100 μm. (D) Percentages of live cells in hollow alginate microfibers immediately after encapsulation, as well as one and 3 days after ($n \geq 3$). Error bars represent ±1 standard deviation. (E) RT-qPCR results showing the fold changes (relative to B2M) of TH and TUBB-3 for control cells, alginate control cells, and encapsulated cells 1 day after manufacturing ($n \geq 1$).

mechanical properties and degradation rates of the models, with alginate hydrogels suspended in maintenance media capable of surviving for multiple weeks.[16,25]

To better understand the genetic implications of the manufacturing process and encapsulating cells into 3D tubular structures, reverse-transcription (RT) quantitative polymerase chain reactions (qPCR) were used to analyze the gene expressions of tyrosine hydroxylase (TH) and tubulin beta 3 class III (TUBB-3) relative to the endogenous control beta-2 microglobulin (B2M). TH and TUBB-3 are good target genes to understand the health and functionality of neural cells; TH encodes for the rate-limiting enzyme tyrosine hydroxylase, which converts tyrosine during the creation of catecholamines, including dopamine.[26,27] TUBB-3 is involved with multiple aspects of cell health and behavior, including forming the cytoskeleton and neurogenesis.[28,29] Analyzing the expression of these genes can give vital cues as to how dopaminergic neural N27 cells are behaving 1 day after manufacturing in hollow alginate microfibers, which is a key factor to designing BBB models that allow for efficient and accurate modeling of BBB.

Fabrication of hollow alginate microfibers: Microfibers were fabricated using a five-inlet microfluidic device and were gathered in a $CaCl_2{\cdot}2H_2O$ bath to ensure that they were strong enough to survive handling. As seen in Figure 2, fibers were fabricated with multiple flow rate ratios (FRRs) to better understand the interactions between the core, prepolymer, and sheath fluids within the microfluidic device and how they affect the final dimensions of the microfibers; these FRRs were (A) 200:150:300, (B) 200:100:300, and (C) 600:250:300 μL/min. (core/prepolymer/sheath). As seen in Figure 2D, increasing the prepolymer solution by 50 μL/min between FRRs A and B but holding all other solutions steady led to an increase in the wall thickness and in the overall width of the fiber. Similarly, minimizing the flow rate differential between the core and prepolymer solutions led to a smoother, more reproducible fiber, as can be observed in the higher error bars seen in the wall and total measurements for FRRs B and C, respectively. However, FRR C showed the widest walls and the most consistent shape; additionally, previous work has shown an inverse relationship between the time the cells are inside the microfluidic device and the overall cell viability after encapsulation.[18] For these reasons, FRR C was chosen for further experiments including cells.

Cell viability in hollow microfibers: Cells were encapsulated within the walls of hollow alginate microfibers, and were observed using CellTracker Green CMFDA and propidium iodide to stain live and dead cells, respectively (Figure 3A–C). As seen in Figure 3D, approximately 65% of cells inside the walls of the hollow microfibers were still alive immediately after encapsulation, a number that did not change significantly throughout the three-day observation. This indicates that conditions within the microfibers are conducive to cell health, and that the fiber boundaries can allow sufficient diffusion across the borders to allow an influx of nutrients and an efflux of waste. Such results are promising for the success of longer-term studies, which will be necessary to create a function BBB model.

Cellular genetic changes after manufacturing: To understand the effects of alginate and the encapsulation process on the genetic expressions of N27 cells, RT-qPCR was performed on untreated control cells, alginate control cells, and encapsulated cells (Figure 3E) 1 day after encapsulation. Alginate control cells were mixed with alginate and put into the syringe as part of the encapsulation experiment, but were not put through the microfluidic device, and were added directly into maintenance media instead.

Cells were analyzed for expressions of the genes TH and TUBB-3 1 day after the encapsulation. The alginate control

https://doi.org/10.1021/acsmacrolett.1c00159
ACS Macro Lett. 2021, 10, 732–736

showed highly elevated amounts of TH, indicating that the N27s had a higher level of tyrosine hydroxylase synthesis for dopamine creation than either the control or the encapsulated cells, which were very similar in terms of TH expression. This indicates that while there is an upregulation that occurs when the cells are in contact with ungelled sodium alginate solutions, the process of ionic cross-linking and encapsulation into calcium alginate hydrogels counteracts this effect to leave N27 cells with TH levels similar to that of the untreated control. This observation is also seen in literature, when mouse embryonic stem cells (mESCs) encapsulated into 2% alginate beads for 18 days showed only slightly raised levels of TH expression than the control.[25]

TUBB-3 levels were suppressed after the addition of alginate, which was also observed in past works on adult hippocampal progenitor stem cells using immunocytochemistry to study β-III tubulin levels.[30] Since TUBB-3 is related neurogenesis and formation of the cytoskeleton, downregulation in these samples indicates that alginate negatively affects cells' ability to perform healthy cellular activities. This is a trend that is continued in encapsulated cells, indicating that the encapsulation process and the situation within the microfibers further inhibits neurogenesis and cytoskeleton formation. Similar results were observed after long-term (7 day) encapsulation of mouse embryonic stem cells in 400 μm diameter alginate beads.[25] This indicates that the microenvironment within the hollow fibers could be improved to be more cell-friendly; this can be accomplished by incorporating extracellular matrix (ECM) components, such as collagen, into the hydrogels.[16]

This work aims to address a crucial need for a BBB model to expedite the understanding of the active molecular transport that occurs between the circulatory system and the central nervous system by studying and validating a novel manufacturing process for encapsulating N27 cells into the walls of hollow fibers. The manufacturing process in this study shows great promise for the fabrication of hollow microfibers with varying wall thicknesses and diameters. Additionally, they show promise for sustaining the lives of encapsulated cells, indicating that sufficient diffusion can take place to bring nutrients into and waste out of the cell walls. However, the genetic responses of encapsulated cells shows that the hollow fibers could be modulated to induce more favorable conditions within the fibers; this could be easily accomplished by either using fibers with thinner walls, thereby necessitating diffusion-based transport of nutrients and waste to and from the cells. To create a feasible BBB model, future work can build off of this manufacturing technique to study long-term encapsulation, cellular proliferation and growth, and cocultures with endothelial and pericyte cells.

■ ASSOCIATED CONTENT

Supporting Information

The Supporting Information is available free of charge at https://pubs.acs.org/doi/10.1021/acsmacrolett.1c00159.

Materials and methods (PDF)

■ AUTHOR INFORMATION

Corresponding Author

Nicole N. Hashemi − *Department of Mechanical Engineering and Department of Biomedical Sciences, Iowa State University, Ames, Iowa 50011, United States;* orcid.org/0000-0001-8921-7588; Email: nastaran@iastate.edu

Authors

Marilyn C. McNamara − *Department of Mechanical Engineering, Iowa State University, Ames, Iowa 50011, United States*

Saurabh S. Aykar − *Department of Mechanical Engineering, Iowa State University, Ames, Iowa 50011, United States*

Reza Montazami − *Department of Mechanical Engineering, Iowa State University, Ames, Iowa 50011, United States;* orcid.org/0000-0002-8827-0026

Complete contact information is available at: https://pubs.acs.org/10.1021/acsmacrolett.1c00159

Author Contributions

M.C.M. wrote the initial draft of the manuscript and, with S.S.A., performed the experiments for the study. R.M. and N.N.H. funded and directed the work. All authors read and discussed the manuscript.

Funding

This work was partially supported by the Office of Naval Research (ONR) Grant N000141612246, ONR Grant N000141712620, and the National Science Foundation Grant 2014346.

Notes

The authors declare no competing financial interest.

■ ACKNOWLEDGMENTS

We thank Dr. Farrokh Sharifi, Dr. Alex Wrede, Dr. Rajeendra Pemathilaka, Kelli R. Williams, and Dr. Jie Luo for their continued support. Dr. Anumantha Kanthasamy kindly supplied the rat dopaminergic neural cells (N27s).

■ REFERENCES

(1) Carter, A. M. Animal Models of Human Placentation - A Review. *Placenta* **2007**, *28*, S41−S47.

(2) Furtado, D.; Bjornmalm, M.; Ayton, S.; Bush, A. I.; Kempe, K.; Caruso, F. Overcoming the Blood-Brain Barrier: The Role of Nanomaterials in Treating Neurological Diseases. *Adv. Mater.* **2018**, *30* (46), 1801362.

(3) Wrede, A. H.; Shah, A.; McNamara, M. C.; Montazami, R.; Hashemi, N. N. Controlled positioning of microbubbles and induced cavitation using a dual-frequency transducer and microfiber adhesion techniques. *Ultrason. Sonochem.* **2018**, *43*, 114−119.

(4) Wrede, A. H.; Luo, J.; Montazami, R.; Kanthasamy, A.; Hashemi, N. N. How do neuroglial cells respond to ultrasound induced cavitation? *AIP Adv.* **2021**, *11* (1), 015314.

(5) Miao, R.; Xia, L.-Y.; Chen, H.-H.; Huang, H.-H.; Liang, Y. Improved Classification of Blood−Brain Barrier Drugs Using Deep Learning. *Sci. Rep.* **2019**, *9* (1), 8802−8813.

(6) Osipova, E. D.; Komleva, Y. K.; Morgun, A. V.; Lopatina, O. L.; Panina, Y. A.; Olovyannikova, R. Y.; Vais, E. F.; Salmin, V. V.; Salmina, A. B. Designing in vitro Blood−Brain Barrier Models Reproducing Alterations in Brain Aging. *Front. Aging Neurosci.* **2018**, *10*, 234.

(7) DeStefano, J. G.; Jamieson, J. J.; Linville, R. M.; Searson, P. C. Benchmarking in vitro tissue-engineered blood−brain barrier models. *Fluids Barriers CNS* **2018**, *15* (1), 32.

(8) Aykar, S. S.; Reynolds, D. E.; McNamara, M. C.; Hashemi, N. N. Manufacturing of poly (ethylene glycol diacrylate)-based hollow microvessels using microfluidics. *RSC Adv.* **2020**, *10* (7), 4095−4102.

(9) Sechi, D.; Greer, B.; Johnson, J.; Hashemi, N. N. Three-Dimensional Paper-Based Microfluidic Device for Assays of Protein and Glucose in Urine. *Anal. Chem.* **2013**, *85* (22), 10733−10737.

(10) Pemathilaka, R. L.; Reynolds, D. E.; Hashemi, N. N. Drug transport across the human placenta: review of placenta-on-a-chip and previous approaches. *Interface Focus* **2019**, *9*, 20190031.
(11) Pemathilaka, R. L.; Reynolds, D. E.; Hashemi, N. N. Maternally administered naltrexone and its major active metabolite 6*β*-naltrexol transport across the placental barrier in vitro. *bioRxiv* **2020**, na.
(12) Pemathilaka, R. L.; Caplin, J. D.; Aykar, S. S.; Montazami, R.; Hashemi, N. N. Placenta-on-a-Chip: In Vitro Study of Caffeine Transport across Placental Barrier Using Liquid Chromatography Mass Spectrometry. *Glob. Chall.* **2019**, *3* (3), 1800112.
(13) Hashemi, N.; Lackore, J. M.; Sharifi, F.; Goodrich, P. J.; Winchell, M. L.; Hashemi, N. N. A paper-based microbial fuel cell operating under continuous flow condition. *Technology* **2016**, *4* (2), 98−103.
(14) Chen, B.; Tian, F.; Hashemi, N. N.; McNamara, M. C.; Cho, M. Characterization of Correlated Calcium Dynamics in Astrocytes in PCL Scaffold: Application of Wavelet Transform Coherence. *J. Mater. Sci. Eng.* **2018**, *7* (3), 2169−0022.
(15) Bai, Z.; Mendoza Reyes, J. M.; Montazami, R.; Hashemi, N. On-chip development of hydrogel microfibers from round to square/ribbon shape. *J. Mater. Chem. A* **2014**, *2*, 4878.
(16) McNamara, M. C.; Sharifi, F.; Wrede, A. H.; Kimlinger, D. F.; Thomas, D.-G.; Vander Wiel, J. B.; Chen, Y.; Montazami, R.; Hashemi, N. N. Microfibers as Physiologically Relevant Platforms for Creation of 3D Cell Cultures. *Macromol. Biosci.* **2017**, *17* (12), 1700279.
(17) McNamara, M. C.; Pretzer, R. J.; Montazami, R.; Hashemi, N. N. Shear at Fluid-Fluid Interfaces Affects the Surface Topologies of Alginate Microfibers. *Clean Technologies* **2019**, *1* (1), 265−272.
(18) McNamara, M. C.; Sharifi, F.; Okuzono, J.; Montazami, R.; Hashemi, N. N. Microfluidic Manufacturing of Alginate Fibers with Encapsulated Astrocyte Cells. *ACS Appl. Bio Mater.* **2019**, *2* (4), 1603−1613.
(19) McNamara, M. C.; Niaraki-Asli, A. E.; Guo, J.; Okuzono, J.; Montazami, R.; Hashemi, N. N. Enhancing the Conductivity of Cell-Laden Alginate Microfibers With Aqueous Graphene for Neural Applications. *Front. Mater.* **2020**, *7*, 61.
(20) Sharifi, F.; Patel, B. B.; McNamara, M. C.; Meis, P. J.; Roghair, M. N.; Lu, M.; Montazami, R.; Sakaguchi, D. S.; Hashemi, N. N. Photo-Cross-Linked Poly(ethylene glycol) Diacrylate Hydrogels: Spherical Microparticles to Bow Tie-Shaped Microfibers. *ACS Appl. Mater. Interfaces* **2019**, *11* (20), 18797−18807.
(21) Sharifi, F.; Patel, B. B.; Dzuilko, A. K.; Montazami, R.; Sakaguchi, D. S.; Hashemi, N. Polycaprolactone Microfibrous Scaffolds to Navigate Neural Stem Cells. *Biomacromolecules* **2016**, *17* (10), 3287−3297.
(22) Patel, B. B.; Sharifi, F.; Stroud, D. P.; Montazami, R.; Hashemi, N. N.; Sakaguchi, D. S. 3D Microfibrous Scaffolds Selectively Promotes Proliferation and Glial Differentiation of Adult Neural Stem Cells: A Platform to Tune Cellular Behavior in Neural Tissue Engineering. *Macromol. Biosci.* **2019**, *19* (2), 1800236.
(23) Sharifi, F.; Kurteshi, D.; Hashemi, N. Designing highly structured polycaprolactone fibers using microfluidics. *J. Mech. Behav. Biomed. Mater.* **2016**, *61*, 530−540.
(24) Sharifi, F.; Bai, Z.; Montazami, R.; Hashemi, N. N. Mechanical and physical properties of poly(vinyl alcohol) microfibers fabricated by a microfluidic approach. *RSC Adv.* **2016**, *6* (60), 55343−55353.
(25) Bozza, A. Alginate-Based Hydrogels for Central Nervous System Tissue Regeneration. *Ph.D. Thesis*, University of Trento, Trento, Italy, 2014.
(26) Zhang, D.; Kanthasamy, A.; Anantharam, V.; Kanthasamy, A. Effects of Manganese on Tyrosine Hydroxylase (TH) Activity and TH-phosphorylation in a Dopaminergic Neural Cell Line. *Toxicol. Appl. Pharmacol.* **2011**, *254* (2), 65−71.
(27) Alam, G.; Richardson, J. R. Regulation of tyrosine hydroxylase: relevance to Parkinson's disease. In *Genetics, Neurology, Behavior, and Diet in Parkinson's Disease: The Neuroscience of Parkinson's Disease*; Martin, C. R., Preedy, V. R., Eds. Elsevier: United Kingdom, 2020; Vol. 2, pp 51−66.
(28) Shao, Q.; Yang, T.; Huang, H.; Majumder, T.; Khot, B. A.; Khouzani, M. M.; Alarmanazi, F.; Gore, Y. K.; Liu, G. Disease-associated mutations in human TUBB3 disturb netrin repulsive signaling. *PLoS One* **2019**, *14* (6), No. e0218811.
(29) Hong, Y. B.; Lee, J. H.; Park, H. J.; Choi, Y.-R.; Hyun, Y. S.; Park, J. H.; Koo, H.; Chung, K. W.; Choi, B.-O. A family with axonal sensorimotor polyneuropathy with TUBB3 mutation. *Mol. Med. Rep.* **2015**, *11* (4), 2729−2734.
(30) Patel, B. B.; McNamara, M. C.; Pesquera-Colom, L. S.; Kozik, E. M.; Okuzonu, J.; Hashemi, N. N.; Sakaguchi, D. S. Recovery of Encapsulated Adult Neural Progenitor Cells from Microfluidic-Spun Hydrogel Fibers Enhances Proliferation and Neuronal Differentiation. *ACS Omega* **2020**, *5*, 7910−7918.

https://doi.org/10.1021/acsmacrolett.1c00159
ACS Macro Lett. 2021, 10, 732−736